Progress In Electromagnetics Research, PIER 32, 317–356, 2001

COMPUTATIONAL ASPECTS OF THE CELL METHOD IN ELECTRODYNAMICS

M. Marrone

DEEI
Università di Trieste, Via Valerio 10
34127 Trieste, Italy

Abstract—A desire to unify the mathematical description of many physical theories, such as electrodynamics, mechanics, thermal conduction, has led us to understand that global (=*integral*) physical variables of each theory can be associated to spatial geometrical elements such as points, lines, surfaces, volumes and temporal geometrical elements such as instants and intervals. This association has led us to build a space-time classification diagram of variables and equations for each theory. Moreover, the possibility to express physical laws directly in a finite rather than differential form has led to the development of a computational methodology called *Cell Method* [12]. This paper discusses some practical aspects of this method and how it may overcome some of the main limitations of FDTD method in electrodynamics. Moreover, we will provide some numerical examples to compare the two methodologies.

1. INTRODUCTION

Several numerical methods to find solutions to Maxwell's equations have been proposed over the years. One of them, possibly the most common and widespread, is the finite-difference time-domain (FDTD) method initially proposed by Yee [2] in 1966. Many studies have been carried out on this method since then (see for example

[11]). In particular, many efforts have been directed to overcoming restrictions in the FDTD method, such as the use of Cartesian orthogonal grids. The main techniques can be divided into two groups arising, respectively, from the differential and the integral formulation of Maxwell's equations:

- *Differential formulation.* One of the first methods using this formulation is the FDTD method in generalized nonorthogonal coordinates proposed by Holland [4] and then used, with some modifications, by others [5, 6, 10].
- *Integral formulation.* In this context we can find many works: some of them are based on Delaunay-Voronoi grids [7, 9], others on grids made by cells with more general shapes [8].

The general goal has been to arrive at a methodology which has the following features [8]:

(i) Allows the use of unstructured non-orthogonal grids.
(ii) Allows different types of cells (tetrahedral, cubic, etc.).
(iii) Recovers the FDTD method when orthogonal grids are used.
(iv) Preserves charge or divergence locally (and globally).
(v) Conditionally stable.
(vi) Non-dispersive.
(vii) Non-dissipative.
(viii) Accurate for non-orthogonal grids.

In this paper, we will describe a method, dubbed *Cell Method*, that incorporates the features (i)–(v) and (viii) above (items (vi)–(vii) have not been analyzed). The Cell Method is based on a formulation strictly related to the integral formulation of Maxwell's equations; it uses global variables of the electrodynamic fields (fluxes Φ,Ψ, voltages V,F, currents I, charge Q_c) rather than differential ones (field vectors $\mathbf{B}$, $\mathbf{D}$, $\mathbf{E}$, $\mathbf{H}$, current density $\mathbf{J}$, charge density ρ). Moreover, we will illustrate some results obtained using Cell Method, and include a comparison against results from the FDTD method and from a full modal expansion.

2. THEORETICAL ASPECTS OF THE CELL METHOD

2.1. Space-Time Structure

The cell method is based, as the first step, on a space-time structure that consists of two spatial geometrical structures:

- Primal spatial grid G, defined by the set of primal elements $G = \{P, L, S, V\}$ that are points P, lines L, surfaces S, volumes V.

- Dual spatial grid $\tilde{G}$, defined by the set of dual elements $\tilde{G} = \{\tilde{P}, \tilde{L}, \tilde{S}, \tilde{V}\}$ that are points $\tilde{P}$, lines $\tilde{L}$, surfaces $\tilde{S}$, volumes $\tilde{V}$.

Each spatial grid is characterized by a cell complex. A generic cell can be a hexahedron, a tetrahedron, or other. The distinction between *primal* and *dual* grids arises from the need for bijective mappings between the elements: $P \leftrightarrow \tilde{V}$,$L \leftrightarrow \tilde{S}$, $S \leftrightarrow \tilde{L}$,$V \leftrightarrow \tilde{P}$. For example, let us take a very simple kind of cell: the regular hexahedron; a complex of which characterizes an orthogonal Cartesian grid. Using two Cartesian grids, respectively as primal and dual grid, with the points $\tilde{P}$ in a barycentric position to the volumes V, it is possible to achieve a cell complex; in figure 1 a cell pair made by two spatial

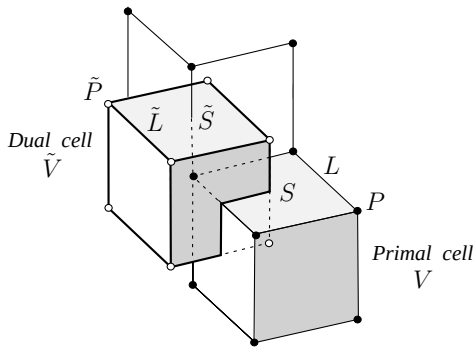

Figure 1. Pair of primal and dual spatial cells.

cubic cells is shown. The bijective mappings between the geometrical elements of cells in figure 1 are shown in figure 2.

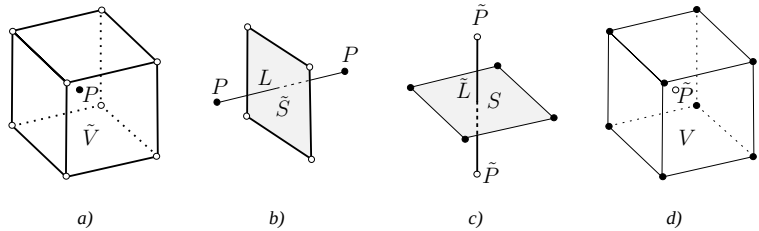

Figure 2. Biunivocal mappings between primal and dual geometrical elements.

Since we are working in time-domain, we also need two temporal geometrical structures:

- Temporal primal grid G_T, defined by the set of primal elements $G_T = \{I, T\}$ that are time instant I, time intervals T.
- Temporal dual grid $\tilde{G}_T$, defined by the set of dual elements $\tilde{G}_T = \{I, T\}$ that are time instant $\tilde{I}$, time intervals $\tilde{T}$.

Between the elements of the two temporal grids the bijective mappings: $I \leftrightarrow \tilde{T}, T \leftrightarrow \tilde{I}$ are also necessary. As spatial grids permit a useful space subdivision in spatial cells likewise temporal grids permit a time axes subdivision in time cells. A time axis, on which a pair of primal and dual temporal grids is built, is shown in figure 3.

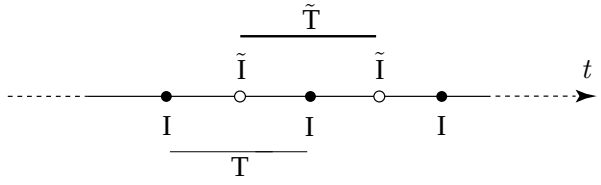

Figure 3. Primal and dual time cells.

2.2. Orientation of Geometrical Elements

We use an inner or an outer orientation for respectively primal or dual spatial elements, as in figure 4.

Moreover we use the following notation, referred in this case to a surface elements:

- **S** indicates a generic oriented surface element.
- S indicates a generic non oriented surface element or its size.
- **s** indicates a specific oriented surface element.
- s indicates a specific non oriented surface element or its size.

2.3. Physical Global Variables of Electrodynamics

Let us define the following physical variables on the space-time structure we have just created:

- **Electric voltage impulse** $\mathcal{V}[\mathbf{L}, \mathbf{T}]$, associated to primal lines **L** and to primal time intervals **T**.
- **Magnetic flux** $\Phi[\mathbf{S}, \mathbf{I}]$, associated to primal surfaces **S** and to primal time instant **I**.

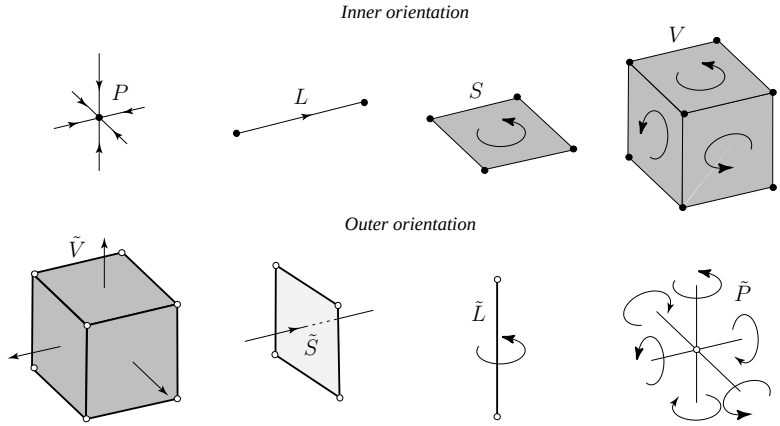

Figure 4. Orientation of geometrical elements of space grids.

- **Magnetic voltage impulse** $\mathcal{F}[\tilde{\mathbf{L}}, \tilde{\mathbf{T}}]$, associated to dual lines $\tilde{\mathbf{L}}$ and to dual time intervals $\tilde{\mathbf{T}}$.
- **Electric flux** $\Psi[\tilde{\mathbf{S}}, \tilde{\mathbf{I}}]$, associated to dual surfaces $\tilde{\mathbf{S}}$ and to dual time instant $\tilde{\mathbf{I}}$.
- **Electric charge content** $Q_{\mathrm{c}}[\tilde{\mathbf{V}}, \tilde{\mathbf{I}}]$, associated to dual volumes $\tilde{\mathbf{V}}$ and to dual time instant $\tilde{\mathbf{I}}$.
- **Electric charge flow** $Q_{\mathrm{f}}[\tilde{\mathbf{S}}, \tilde{\mathbf{T}}]$, associated to dual surfaces $\tilde{\mathbf{S}}$ and to dual time intervals $\tilde{\mathbf{T}}$.

The connection with the integral notation is obvious:

- Electric voltage impulse
$$\mathcal{V}[\mathbf{L}, \mathbf{T}] = \int_T \int_L \mathbf{E} \cdot d\mathbf{l}\, dt$$
- Magnetic flux
$$\Phi[\mathbf{S}, \mathbf{I}] = \int_S \mathbf{B} \cdot d\mathbf{s}$$
- Magnetic voltage impulse
$$\mathcal{F}[\tilde{\mathbf{L}}, \tilde{\mathbf{T}}] = \int_{\tilde{T}} \int_{\tilde{L}} \mathbf{H} \cdot d\mathbf{l}\, dt$$
- Electric flux
$$\Psi[\tilde{\mathbf{S}}, \tilde{\mathbf{I}}] = \int_{\tilde{S}} \mathbf{D} \cdot d\mathbf{s}$$
- Electric charge content
$$Q_{\mathrm{c}}[\tilde{\mathbf{V}}, \tilde{\mathbf{I}}] = \int_{\tilde{V}} \rho dv$$

- Electric charge flow

$$Q_{\mathrm{f}}[\tilde{\mathbf{S}}, \tilde{\mathbf{T}}] = \int_{\tilde{T}} \int_{\tilde{S}} \mathbf{J} \cdot d\mathbf{s}\, dt$$

In order to emphasize the space associations, each variable is indexed by a subscript:
h) If the variable refers to the primal point $\mathbf{p}_h$ or to the dual volume $\tilde{\mathbf{v}}_h$.
α) If the variable refers to the primal line $\mathbf{l}_\alpha$ or to the dual surface $\tilde{\mathbf{s}}_\alpha$.
β) If the variable refers to the primal surface $\mathbf{s}_\beta$ or to the dual line $\tilde{\mathbf{l}}_\beta$.
k) If the variable refers to the primal volume $\mathbf{v}_k$ or to the dual point $\tilde{\mathbf{p}}_k$.
Moreover, each variable is indexed by a prime, to emphasize the time associations. The prime indicates the instant or the interval in which the variable is computed. The prime *n-1/2* indicates the dual time instant $\tilde{\mathbf{t}}_n$ or the corresponding primal time interval τ_n, while the prime n points out the primal time instant $\mathbf{t}_n$ or the corresponding dual time interval $\tilde{\tau}_n$. Briefly we use the following:

$$\begin{aligned}
&\mathcal{V}_\alpha^{n-1/2} \equiv \mathcal{V}[\mathbf{l}_\alpha, \tau_n], && \Phi_\beta^n \equiv \Phi[\mathbf{s}_\beta, \mathbf{t}_n] \\
&\mathcal{F}_\beta^n \equiv \mathcal{F}[\tilde{\mathbf{l}}_\beta, \tilde{\tau}_n], && \Psi_\alpha^{n-1/2} \equiv \Psi[\tilde{\mathbf{s}}_\alpha, \tilde{\mathbf{t}}_n] \\
&Q_{\mathrm{c}_h}^{n-1/2} \equiv Q_{\mathrm{c}}[\tilde{\mathbf{v}}_h, \tilde{\mathbf{t}}_n], && Q_{\mathrm{f}_\alpha}^n \equiv Q_{\mathrm{f}}[\tilde{\mathbf{s}}_\alpha, \tilde{\tau}_n]
\end{aligned}$$

The physical variable associations to the space cells and to the time cells respectively are shown separately in figures 5 and 6.

2.4. Electrodynamic Laws

Now we can express electrodynamic laws in a finite form. It is possible to achieve them exactly from Maxwell's integral equations, but in the following finite form we can see that these laws are only a number of relations joining variables defined on the same kind of grid. In fact: *On primal grids we can express:*

Faraday's law:

$$\Phi_\beta^n = \Phi_\beta^{n-1} - \sum_\alpha c_{\beta\alpha} \mathcal{V}_\alpha^{n-1/2} \tag{1}$$

that is a *circulation law on* $\mathbf{s}_\beta$. The incidence number $c_{\beta\alpha}$ is 0, if the line $\mathbf{l}_\alpha$ does not belong to the border of the surface $\mathbf{s}_\beta$, otherwise it is 1 o -1 according to whether the orientation of $\mathbf{l}_\alpha$ is or is not compatible with the orientation of $\mathbf{s}_\beta$.

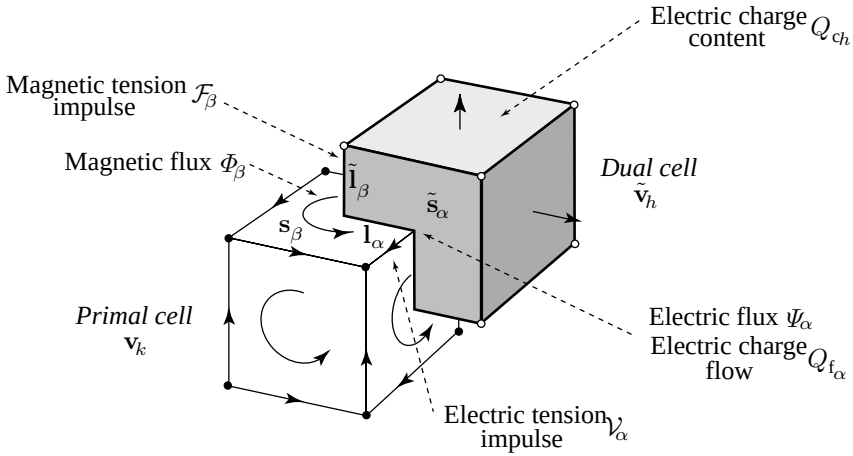

Figure 5. Physical variables on spatial cells.

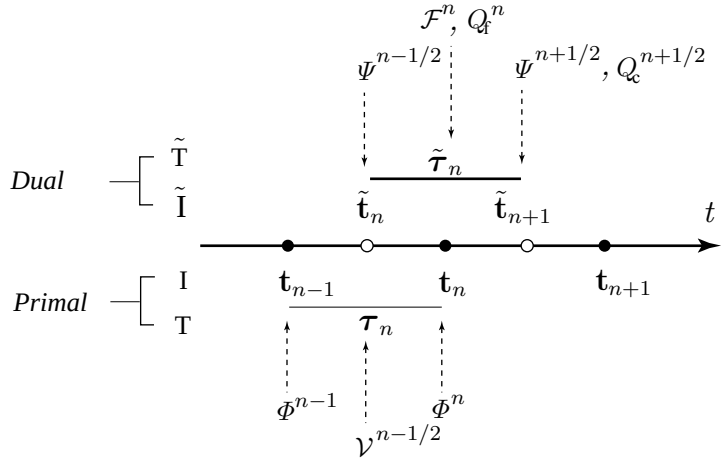

Figure 6. Physical variables on time cells.

Gauss' law (magnetism):

$$\sum_{\beta} d_{k\beta}\Phi_{\beta}^{n} = 0 \tag{2}$$

that is a *balance law on* $\mathbf{v_k}$. The incidence number $d_{k\beta}$ is 0, if the surface $\mathbf{s}_\beta$ is not a face of the volume $\mathbf{v_k}$, otherwise it is 1 o -1 according to whether the orientation of $\mathbf{s}_\beta$ is or is not compatible with the orientation of $\mathbf{v_k}$. *On dual grids we can express:*

Maxwell-Ampère's law:

$$\Psi_{\alpha}^{n+1/2} = \Psi_{\alpha}^{n-1/2} + \sum_{\beta} \tilde{c}_{\alpha\beta}\mathcal{F}_{\beta}^{n} - {Q_{\mathrm{f}}}_{\alpha}^{n} \tag{3}$$

that is a *circulation law on* $\tilde{\mathbf{s}}_\alpha$. The incidence number $\tilde{c}_{\alpha\beta}$ is 0, if the dual line $\tilde{\mathbf{l}}_\beta$ does not belong to the border of the surface $\tilde{\mathbf{s}}_\alpha$, otherwise it is 1 or -1 according to whether the orientation of $\tilde{\mathbf{l}}_\beta$ is or is not compatible with the orientation of $\tilde{\mathbf{s}}_\alpha$. The variables ${Q_{\mathrm{f}}}_\alpha$ can be broken down into a sum of two terms: ${Q_{fc}}_\alpha$ conduction charge flow and ${Q_{fi}}_\alpha$ impressed charge flow.

Gauss' law (electricity):

$$\sum_{\alpha} \tilde{d}_{h\alpha}\Psi_{\alpha}^{n-1/2} = {Q_{\mathrm{c}}}_{h}^{n-1/2} \tag{4}$$

that is a *balance law on* $\tilde{\mathbf{v}}_\mathbf{h}$. The incidence number $\tilde{d}_{h\alpha}$ is 0, if the surface $\tilde{\mathbf{s}}_\alpha$ is not a face of the volume $\tilde{\mathbf{v}}_\mathbf{h}$, otherwise it is 1 or -1 according to whether the orientation of $\tilde{\mathbf{s}}_\alpha$ is or is not compatible with the orientation of $\tilde{\mathbf{v}}_\mathbf{h}$.

Charge conservation law:

$${Q_{\mathrm{c}}}_{h}^{n+1/2} = {Q_{\mathrm{c}}}_{h}^{n-1/2} - \sum_{\alpha} \tilde{d}_{h\alpha}{Q_{\mathrm{f}}}_{\alpha}^{n} \tag{5}$$

that is a *balance law on* $\tilde{\mathbf{v}}_\mathbf{h}$. The electrodynamic laws above are topological equations; hence they are independent from shapes and sizes of primal and dual grids. Moreover, they are independent from the material media present in the space domain. From (1), it is possible to obtain (2) and from (3) and (4), it is possible to obtain (5). This fact ensure that the use of equations (1),(3), and (4) preserves divergence.

2.5. Time Approximation

We always choose $\tau_n = \tilde{\tau}_n = \tau$, where $\tau_n = \tau$ is a fixed time interval, and $t_n = n\tau$, $\tilde{t}_n = (n - 1/2)\tau$ where n is an integer number, in order to achieve a second time order approximation [7, 8]. Moreover, for our convenience, we define the following variables that are global only in space:

- **Electric voltage**
$$V_\alpha^{n-1/2} \equiv V[\mathbf{l}_\alpha, \tilde{\mathbf{t}}_\mathbf{n}] \approx \frac{\mathcal{V}[\mathbf{l}_\alpha, \tau_\mathbf{n}]}{\tau_n}$$
- **Magnetic voltage**
$$F_\beta^n \equiv F[\tilde{\mathbf{l}}_\beta, \mathbf{t}_\mathbf{n}] \approx \frac{\mathcal{F}[\tilde{\mathbf{l}}_\beta, \tilde{\tau}_\mathbf{n}]}{\tilde{\tau}_n}$$
- **Electric current**
$$I_\alpha^n \equiv I[\tilde{\mathbf{s}}_\alpha, \mathbf{t}_\mathbf{n}] \approx \frac{Q_\mathrm{f}[\tilde{\mathbf{s}}_\alpha, \tilde{\tau}_\mathbf{n}]}{\tilde{\tau}_\mathbf{n}}$$

With time approximation, the electrodynamic laws become:

Faraday's law:

$$\Phi_\beta^n \approx \Phi_\beta^{n-1} - \tau_n \sum_\alpha c_{\beta\alpha} V_\alpha^{n-1/2} \tag{6}$$

Maxwell-Ampère's law:

$$\Psi_\alpha^{n+1/2} \approx \Psi_\alpha^{n-1/2} + \tilde{\tau}_n \sum_\beta \tilde{c}_{\alpha\beta} F_\beta^n - \tilde{\tau}_n I_\alpha^n \tag{7}$$

The variables I_α^n can be broken down into a sum of two terms: the conduction current $I_{\mathrm{c}\alpha}^n$, and the impressed current $I_{\mathrm{i}\alpha}^n$.

Conservation charge law:

$$Q_{\mathrm{c}h}^{n+1/2} \approx Q_{\mathrm{c}h}^{n-1/2} - \tilde{\tau}_n \sum_\alpha \tilde{d}_{h\alpha} I_\alpha^n \tag{8}$$

2.6. Stability

The electrodynamic laws (6)–(8) are structured in the typical form of a leap-frog algorithm. In order to ensure its numerical stability an upper limitation of the time step $\tau = \tau_n = \tilde{\tau}_n$ is necessary. An interesting useful condition is the following [7, 11]:

$$\tau \leq min \left[min_k \left(\frac{1}{c_k} \sqrt{\frac{2v_k}{\sum_\beta |d_{k\beta}| \frac{s_\beta}{\tilde{l}_\beta}}} \right), min_h \left(\frac{1}{c_h} \sqrt{\frac{2\tilde{v}_h}{\sum_\alpha |\tilde{d}_{h\alpha}| \frac{\tilde{s}_\alpha}{l_\alpha}}} \right) \right] \tag{9}$$

where c_k e c_h are the maximum wave propagation speed, respectively in the primal cells v_k and in the dual cells $\tilde{v}_h$. In the case of Cartesian orthogonal grids, as in the FDTD method, the equation (9) becomes the well-known Courant criteria.

3. THE DELAUNAY-VORONOI METHOD

3.1. Delaunay-Voronoi Grids

3.1.1. Two-Dimensional Extrude Grids

We shall use the name *two-dimensional extrude grids* to refer to all the cases in which three-dimensional grids arise from a process of extrusion of two-dimensional grids along the z-axis. In order to speak about two-dimensional extrude cases it is better, as a first step, to refer to two-dimensional primal and dual grids of origin. For these, since there are no volumes, the bijective mappings: $P \leftrightarrow \tilde{S}$, $L \leftrightarrow \tilde{L}$, $S \leftrightarrow \tilde{P}$ are necessary. Starting from a Delaunay two-dimensional triangular grid, it is possible to build the Voronoi matched grid if:

- The dual points $\tilde{P}$ are the circumcenters of the matching primal surfaces S (triangles).
- The dual lines $\tilde{L}$ are the axes of the matched primal lines L.
- The dual surfaces $\tilde{S}$ are the surfaces with as a border the dual lines surrounding the matched primal points P.

In figure (7a) some primal and dual two-dimensional cells arising from a Delaunay-Voronoi grid are shown. Starting from these grids, by means of a vertical extrude of their own elements, it is possible to achieve some simple three-dimensional grids (called two-dimensional extrude grids). For the purposes of coherence and to satisfy the necessary conditions of bijective mappings: $P \leftrightarrow \tilde{V}$, $L \leftrightarrow \tilde{S}$, $S \leftrightarrow \tilde{L}$, $V \leftrightarrow \tilde{P}$ it follows that:

- The volumes V are the prisms resulting from a vertical extrusion of the primal surfaces S of an arbitrary height h.
- The volumes $\tilde{V}$ are the prisms resulting from a vertical extrusion of the dual surfaces $\tilde{S}$ of a height h.
- The points $\tilde{P}$ are the spherocenters of the matched volumes V. They are the extrude points, of the height $h/2$, of the circumcenters of the primal surfaces S of origin.

In figure 7b an example of the two-dimensional extrude grids, arising from the two-dimensional grid in figure 7a, is shown.

3.1.2. Three-Dimensional Grids

Given a Delaunay tetrahedral grid as primal three-dimensional grid, it is easy to achieve the matching Voronoi grid in the following manner:

- The dual points $\tilde{P}$ are the spherocenters of the matched primal tetrahedral volumes V.
- The dual lines $\tilde{L}$ are the straight lines, orthogonal to the matched primal surfaces S, with as a border the spherocenters of volumes V that have S as face.
- The dual surfaces $\tilde{S}$ are the surfaces lying on a plane which is orthogonal to the matched primal lines L. The $\tilde{S}$ are characterized by the surrounding dual lines $\tilde{L}$ that are orthogonal to the planes with L as part of their border.
- The dual volumes $\tilde{V}$ are characterized by the dual surfaces enveloping the matched primal points P.

An example of three-dimensional Delaunay-Voronoi grid is shown in figure 7c.

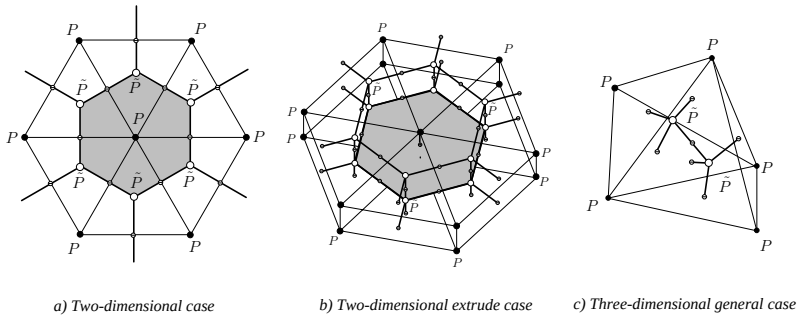

Figure 7. Delaunay-Voronoi grids.

3.1.3. Orthogonality

Besides the bijective mappings $L \leftrightarrow \tilde{S}$, $S \leftrightarrow \tilde{L}$, if there are the orthogonality relations $L \perp \tilde{S}$, $S \perp \tilde{L}$ we will say that *the primal and dual grid are orthogonal to each other.* In this definition the pair of Cartesian orthogonal grids in figure 1 are orthogonal between them, as Delaunay-Voronoi grids are.

3.1.4. Cell Method and Delaunay-Voronoi Grids

Let us define *Delaunay-Voronoi Method* the cell method applied to Delaunay-Voronoi grids. The use of Delaunay-Voronoi grids brings the following advantages:

(i) The tetrahedral primal grid is adaptable to structures with particular geometries that are hard to model by structured cubic grids.
(ii) It is possible to refine the grids only in the zones of interest, with no need for global refining that would produce grids with too many cells.

Disadvantages are:

(i) It is necessary to use good grid generators (the reason will be clear later).
(ii) Unstructured grids require more extensive calculations.

It should be noted that the Delaunay-Voronoi Method is actually not a new method, but simply a slightly different version of other methods [7, 9].

3.2. Constitutive Equations

Constitutive equations are the only relations connecting primal and dual variables.

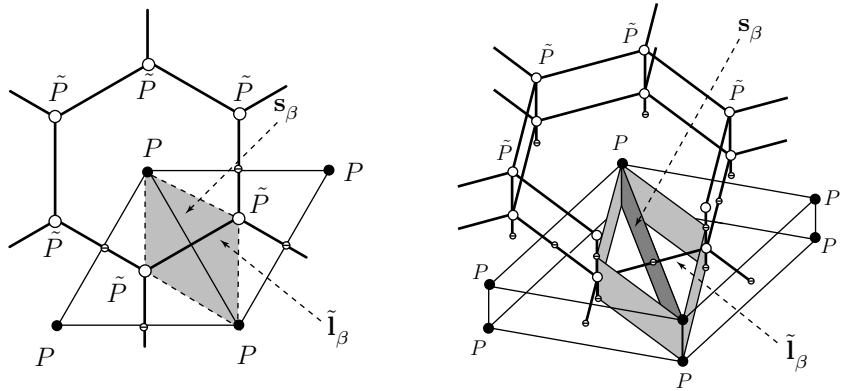

a) Top view *b)Axonometric view*

Figure 8. Uniformity field zone for the magnetic constitutive equation.

They can be expressed by the following:

(a) Magnetic constitutive equation

Given a primal surface s_β, the matched dual line $\tilde{l}_\alpha$ and the primal time instant t_n, we seek a relation between $\Phi^n_\beta \equiv \Phi[\mathbf{s}_\beta, \mathbf{t_n}]$ and

$F^n_\beta \equiv F[\tilde{\mathbf{l}}_\beta](\mathbf{t_n})$. If there is a uniform magnetic field and a uniform permeability μ in a zone containing s_β and $\tilde{l}_\beta$, as in figure 8 for a two-dimensional extrude case and, since $s_\beta \perp \tilde{l}_\beta$, the magnetic constitutive equation may be expressed as:

$$\frac{\Phi[\mathbf{s}_\beta, \mathbf{t_n}]}{s_\beta} = \mu \frac{F[\tilde{\mathbf{l}}_\beta](\mathbf{t_n})}{\tilde{l}_\beta} \quad or \quad \frac{\Phi^n_\beta}{s_\beta} = \mu \frac{F^n_\beta}{\tilde{l}_\beta} \tag{10}$$

(b) Electric constitutive equation

Given a dual surface $\tilde{s}_\alpha$, the matched primal line l_β and the dual time instant $\tilde{t}_n$, we seek a relation between $\Psi^{n-1/2}_\alpha \equiv \Psi[\tilde{\mathbf{s}}_\alpha, \tilde{\mathbf{t}}_\mathbf{n}]$ and $V^{n-1/2}_\alpha \equiv V[\mathbf{l}_\alpha](\tilde{\mathbf{t}}_\mathbf{n})$. If there is a uniform electric field and a uniform dielectric constant ε in a zone containing $\tilde{s}_\alpha$ and l_α, since $\tilde{s}_\alpha \perp l_\alpha$ the electric constitutive equation may be expressed as:

$$\frac{\Psi[\tilde{\mathbf{s}}_\alpha, \tilde{\mathbf{t}}_\mathbf{n}]}{\tilde{s}_\alpha} = \varepsilon \frac{V[\mathbf{l}_\alpha](\tilde{\mathbf{t}}_\mathbf{n})}{l_\alpha} \quad or \quad \frac{\Psi^{n+1/2}_\alpha}{\tilde{s}_\alpha} = \varepsilon \frac{V^{n+1/2}_\alpha}{l_\alpha} \tag{11}$$

(c) Ohm's law:

Given a dual surface $\tilde{s}_\alpha$, the matched primal line l_β and the dual time instant $\tilde{t}_n$, we seek a relation between $I^n_\alpha \equiv I[\tilde{\mathbf{s}}_\alpha](\mathbf{t_n})$ and $V^n_\alpha \equiv V[\mathbf{l}_\alpha](\mathbf{t_n})$. If there is a uniform electric field and a uniform conductivity constant σ in a zone containing $\tilde{s}_\alpha$ and l_α, since $\tilde{s}_\alpha \perp l_\alpha$ Ohm's law may be expressed as:

$$\frac{I[\tilde{\mathbf{s}}_\alpha](\mathbf{t_n})}{\tilde{s}_\alpha} = \sigma \frac{V[\mathbf{l}_\alpha](\mathbf{t_n})}{l_\alpha} \quad or \quad \frac{I^n_\alpha}{\tilde{s}_\alpha} = \sigma \frac{V^n_\alpha}{l_\alpha} \tag{12}$$

Let us note that the variable $V^n_\alpha \equiv V[\mathbf{l}_\alpha](\mathbf{t_n})$, in Ohm's law, does not exist on the structures just created, because it is matched to the dual time instant $\tilde{t}_n$. Hence it must be estimated by means of some time approximations:

- Explicit approximation

$$V^n \cong aV^{n-1/2} + bV^{n-3/2} + ... \tag{13}$$

with a,b,... numerical coefficients. This approximation needs other limitations on the value τ (as $\tau < \frac{\varepsilon}{\sigma}$), besides the limit (9), to ensure the stability of the leap-frog algorithm.

- Implicit approximation

$$V^n \cong ... + aV^{n+1/2} + bV^{n-1/2} + ... \tag{14}$$

with a,b,... numerical coefficients. This approximation does not require the limitations of explicit approximation. The assumption

$$V^n \cong \frac{V^{n+1/2} + V^{n-1/2}}{2} \tag{15}$$

used in the FDTD method [11], is an example of semi-implicit approximation. The Ohm's law with semi-implicit approximation becomes

$$\frac{I_\alpha^n}{\tilde{s}_\alpha} = \sigma \frac{V_\alpha^{n+1/2} + V_\alpha^{n-1/2}}{2\ l_\alpha} \tag{16}$$

3.2.1. Considerations on Maxwell-Ampère's Law

Using the electric constitutive equation (11) and the Ohm's law (16), the Maxwell-Ampère's law becomes

$$\Psi_\alpha^{n+1/2} = \Psi_\alpha^{n-1/2} + \tilde{\tau}_n \sum_\beta \tilde{c}_{\alpha\beta} F_\beta^n - \tilde{\tau}_n I_{\mathrm{i}\alpha}^n - \tilde{\tau}_n \frac{\sigma}{2\varepsilon} (\Psi_\alpha^{n+1/2} + \Psi_\alpha^{n-1/2}) \tag{17}$$

This implicit approximation can be explicitly expressed as

$$\Psi_\alpha^{n+1/2} = \left(\frac{1 - \frac{\tilde{\tau}_n \sigma}{2\varepsilon}}{1 + \frac{\tilde{\tau}_n \sigma}{2\varepsilon}} \right) \Psi_\alpha^{n-1/2} + \left(\frac{\tilde{\tau}_n}{1 + \frac{\tilde{\tau}_n \sigma}{2\varepsilon}} \right) (\sum_\beta \tilde{c}_{\alpha\beta} F_\beta^n - I_{\mathrm{i}\alpha}^n) \tag{18}$$

3.3. Computational Algorithm

Starting from the initial conditions
$I_\alpha^{-1} = 0$, $V_\alpha^{-1/2} = 0 \Rightarrow \Psi_\alpha^{-1/2} = 0$, $F_\beta^0 = 0 \Rightarrow \Phi_\beta^0 = 0$
the variables of the electrodynamic field, generated by an impressed current starting from the initial time instant $n = 0$, can be computed through the following steps:

- Computation of $\Psi_\alpha^{1/2}$ by the Maxwell-Ampère's law (18).
- Computation of $V_\alpha^{1/2}$ by the electric constitutive equations (11) and by any boundary conditions.
- Computation of Φ_β^1 by the Faraday's law (6).
- Computation of F_β^1 by the magnetic constitutive equation (10) and by any boundary conditions.
- Iterate

3.4. Limits of the Delaunay-Voronoi Method

The use of Delaunay-Voronoi grids and, particularly, the use of the spherocenters of the primal volumes as dual points may lead to bad approximations. In two-dimensional extrude cases, for example, if the base of a volume V is an obtuse-angle triangle, it happens that the dual point, which is the spherocenter of V, lies outside V itself. This may lead to bad approximations using the constitutive equations (10)(11)(12). Let us analyze the magnetic constitutive equation (10)

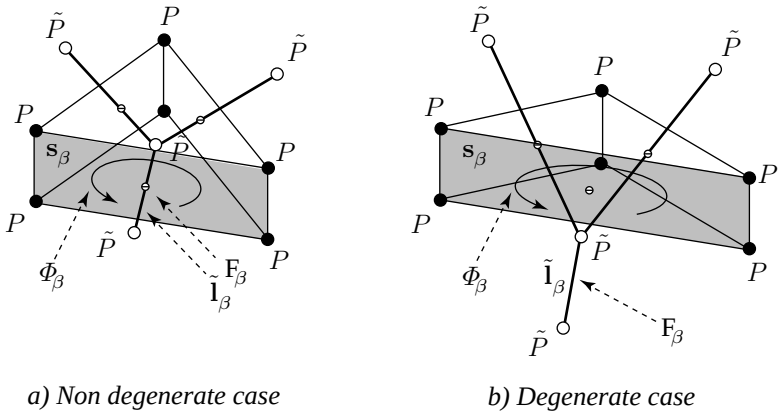

Figure 9. Cases of inner (a) and outer (b) circumcenter respect the primal cell.

applied to the two simple cases in figure 9, where there are two two-dimensional extrude cells: while in case (a) of acute-angle triangle we can think that the relation between Φ_β ed F_β is well approximated by (10), we cannot think the same for case (b), since it is impossible to have a zone of uniformity of B field where there are both s_β and $\tilde{l}_\beta$, as the one in figure 8. Accordingly, to avoid or to limit the situations such as in case (b), it is preferable to have primal two-dimensional grids constituted, as much as possible, by acute-angle triangles, and even better if equilateral. In the three-dimensional case, the situation is analogous: it is better to have as much as possible equilateral tetrahedrons. These are the main reasons why it is better that primal triangular grids are Delaunay grids. However, this condition is not sufficient to ensure that triangles, or tetrahedrons, are all equilateral. Consequently, the efficacy of the Delaunay-Voronoi Method depends the use of very good grid-generators. Moreover, it is not possible to use this methodology for anisotropic situations, a further limitation for

the Delaunay-Voronoi Method.

4. THE MICROCELL METHOD

4.1. Introduction

The limitations of the previous section lead to:

(i) Use more general grids (possibly not orthogonal between them)
(ii) Find other constitutive equations to adapt them to item 1.

One idea is to use the same kind of previous primal grids but, as dual grids, to use particular grids that we call *barycentric* grids. As in paragraph 3.1 we distinguish extrude cases from more general ones.

4.2. Barycentric Grids

4.2.1. Two-Dimensional Extrude Case

Given a Delaunay two-dimensional triangular grid, it is possible to build the barycentric matched grid if:

- The dual points $\tilde{P}$ are the barycenters of the matched primal surfaces S (triangles).
- The dual lines $\tilde{L}$ are piece-lines made by two straight lines whose contact point is the barycenter of the matched primal line L. The extremes of $\tilde{L}$ are the dual points $\tilde{P}$, barycenters of the surfaces S with the same L as part of their border.
- The dual surfaces $\tilde{S}$ are the surfaces having with as a border the dual lines surrounding the matched primal point P.

In figure 10a a two-dimensional barycentric grid is shown. Now it is possible to build two-dimensional extrude grids in the same way as paragraph 3.1.1., swapping the spherocenters with the barycenters, thus we can achieve the result in figure 10b.

4.2.2. Three-Dimensional Case

Given a primal tetrahedral grid, it is possible to build the matched dual barycentric grid in the following way:

- The dual points $\tilde{P}$ are the barycentres of matched primal volumes V (tetrahedrons).
- The dual lines $\tilde{L}$ are piece-lines made by two straight lines whose contact point is the barycenter of the matched primal surface S. The extremes of $\tilde{L}$ are the dual points $\tilde{P}$, barycenters of the volumes V with the same S as face.

- The dual surfaces $\tilde{S}$ are made by plane microfaces. Each microface is located between the barycenter of the primal line L, matched to the $\tilde{S}$, and the border lines of the $\tilde{S}$ itself, which are the dual lines $\tilde{L}$ matched to the surfaces S with the same L as part of their border.
- The dual volumes $\tilde{V}$ are characterized by the dual surfaces $\tilde{S}$ enveloping the matched primal points P.

An example of three-dimensional barycentric grid is shown in figure 10c.

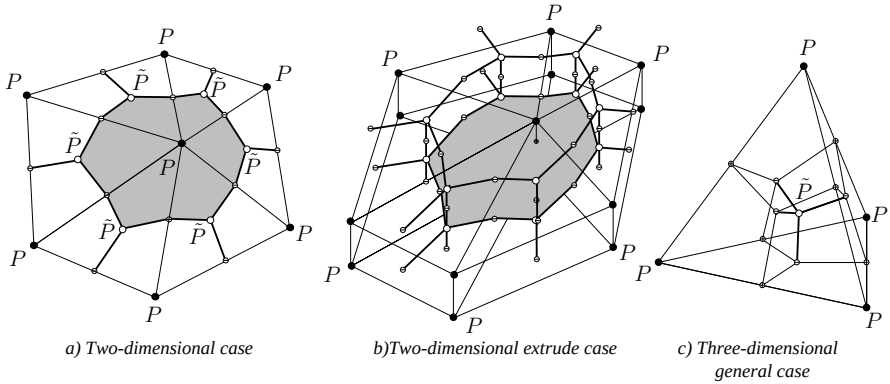

Figure 10. Barycentric grids.

4.3. Microcells

Microcells are elementary cells, with quadrangular shape in two-dimensional cases and hexahedrical shape in three-dimensional cases, and which arise naturally from the use of barycentric dual grids with orthogonal Cartesian or triangular/tetrahedral primal grids. For example, in figure 10a each primal cell is made by 3 quadrangular microcells, while the dual cell by 6 quadrangular microcells; in figure 10c the primal tetrahedral cell is made by 4 hexahedral microcells. We can observe that each primal and dual cell can be broken down into microcells and each microcell belongs, at the same time, to a primal and a dual cell: so microcells are the atomic units of our domain.

4.4. Microcells and the Cell Method

Microcells are the building blocks on which we build a new computational method, the *Microcell Method* or, in the time domain,

the *MCTD method*, for MicroCell in the Time Domain method. It is based on the philosophy and the equations of Cell method, and it uses primal grids with dual barycentric grids.

4.5. Constitutive Equations

Since, in the present case, there is no orthogonality between primal and dual grid, it is obvious that the equations (10)(11)(12) are not useful. Nevertheless, we can still use the idea of a volumetric sampling of the electrodynamic field, that is we could approximate it by means of a set of uniform fields. Since microcells have all the same kind of shape, it seems natural to choose them as zones of uniform field. Hence we establish that in each microcell every field vector (**B**, **H**, **D**, **E**), current vector (**J**) or material feature $(\varepsilon, \mu, \sigma)$ is uniform. Microcells permit to reformulate the known constitutive tensorial equations in a new form using only global variables. In the present paper we will speak only about two-dimensional extrude cases, even if the method is valid for general three-dimensional cases.

4.5.1. Magnetic Constitutive Equation

Let us consider a prismatic three-dimensional primal cell as that in figure 11a, part of a two-dimensional extrude grid. We assume that

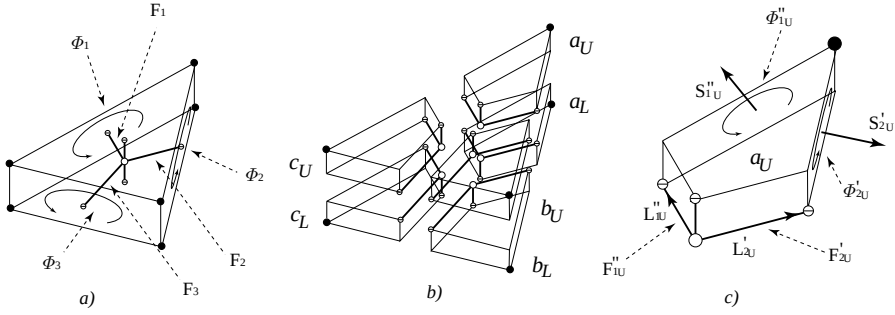

Figure 11. A microcell subdivision of a primal two-dimensional extrude cell.

inside it:

- The field vectors B and H have only x and y-components and they are z-coordinate independent (two-dimensional fields).
- The permeability μ is z-coordinate independent.

Hence, using the tensorial equation $\mathbf{B} = \mu\mathbf{H}$, for the primal cell, we want to express the magnetic constitutive equation in the following form:

$$\begin{cases} \Phi_1 = f_1(F_1, F_2, F_3) \\ \Phi_2 = f_2(F_1, F_2, F_3) \\ \Phi_3 = f_3(F_1, F_2, F_3) \end{cases} \tag{19}$$

where

- The variables Φ are associated to the primal lateral surfaces S (the Φ associated to primal surfaces S z-orthogonal are null).
- The variables F are associated to the straight parts of dual lines lying in the primal cell (F associated to dual lines L z-parallel are null).

Let us divide the primal cell in 6 microcells, as in figure 10b. For the microcell aU in figure 10c let us define:

$$S''_{1Ux} = \mathbf{S''_{1U}} \cdot \mathbf{i} \ , \ S''_{1Uy} = \mathbf{S''_{1U}} \cdot \mathbf{j} \ , \ S'_{2Ux} = \mathbf{S'_{2U}} \cdot \mathbf{i} \ , \ S'_{2Uy} = \mathbf{S'_{12}} \cdot \mathbf{j}$$
$$\tilde{L}''_{1Ux} = \tilde{\mathbf{L}}''_{\mathbf{1U}} \cdot \mathbf{i} \ , \ \tilde{L}''_{1Uy} = \tilde{\mathbf{L}}''_{\mathbf{1U}} \cdot \mathbf{j} \ , \ \tilde{L}'_{2Ux} = \tilde{\mathbf{L}}'_{\mathbf{2U}} \cdot \mathbf{i} \ , \ \tilde{L}'_{2Uy} = \tilde{\mathbf{L}}'_{\mathbf{12}} \cdot \mathbf{j}$$

and since

$$\begin{Bmatrix} \Phi''_{1U} \\ \Phi'_{2U} \end{Bmatrix} = \begin{bmatrix} S''_{1Ux} & S''_{1Uy} \\ S'_{2Ux} & S'_{2Uy} \end{bmatrix} \begin{Bmatrix} B_x \\ B_y \end{Bmatrix} \tag{20}$$

$$\mathbf{B} = \mu\mathbf{H} \tag{21}$$

$$\begin{Bmatrix} F''_{1U} \\ F'_{2U} \end{Bmatrix} = \begin{bmatrix} \tilde{L}''_{1Ux} & \tilde{L}''_{1Uy} \\ \tilde{L}'_{2Ux} & \tilde{L}'_{2Uy} \end{bmatrix} \begin{Bmatrix} H_x \\ H_y \end{Bmatrix} \tag{22}$$

we immediately obtain that

$$\begin{Bmatrix} \Phi''_{1U} \\ \Phi'_{2U} \end{Bmatrix} = \begin{bmatrix} S''_{1Ux} & S''_{1Uy} \\ S'_{2Ux} & S'_{2Uy} \end{bmatrix} \mu \begin{bmatrix} \tilde{L}''_{1Ux} & \tilde{L}''_{1Uy} \\ \tilde{L}'_{2Ux} & \tilde{L}'_{2Uy} \end{bmatrix}^{-1} \begin{Bmatrix} F''_{1U} \\ F'_{2U} \end{Bmatrix} \tag{23}$$

or

$$\begin{Bmatrix} \Phi''_{1U} \\ \Phi'_{2U} \end{Bmatrix} = [M_\mu]^{aU} \begin{Bmatrix} F''_{1U} \\ F'_{2U} \end{Bmatrix} \tag{24}$$

that is the constitutive equation of the microcell. In this way we can express the constitutive equations of all the microcells in the primal cell:

$$\begin{Bmatrix} \Phi''_{1U} \\ \Phi'_{2U} \end{Bmatrix} = [M_\mu]^{aU} \begin{Bmatrix} F''_{1U} \\ F'_{2U} \end{Bmatrix}, \begin{Bmatrix} \Phi''_{1L} \\ \Phi'_{2L} \end{Bmatrix} = [M_\mu]^{aL} \begin{Bmatrix} F''_{1L} \\ F'_{2L} \end{Bmatrix} \tag{25}$$

$$\left\{ \begin{array}{c} \Phi_{2U}^{''} \\ \Phi_{3U}^{'} \end{array} \right\} = [M_\mu]^{bU} \left\{ \begin{array}{c} F_{2U}^{''} \\ F_{3U}^{'} \end{array} \right\}, \left\{ \begin{array}{c} \Phi_{2L}^{''} \\ \Phi_{3L}^{'} \end{array} \right\} = [M_\mu]^{bL} \left\{ \begin{array}{c} F_{2L}^{''} \\ F_{3L}^{'} \end{array} \right\} \quad (26)$$

$$\left\{ \begin{array}{c} \Phi_{3U}^{''} \\ \Phi_{1U}^{'} \end{array} \right\} = [M_\mu]^{cU} \left\{ \begin{array}{c} F_{3U}^{''} \\ F_{1U}^{'} \end{array} \right\}, \left\{ \begin{array}{c} \Phi_{3L}^{''} \\ \Phi_{1L}^{'} \end{array} \right\} = [M_\mu]^{cL} \left\{ \begin{array}{c} F_{3L}^{''} \\ F_{1L}^{'} \end{array} \right\} \quad (27)$$

Since each upper microcell (U) is equal to its respective lower microcell (L) we obtain that: $[M_\mu]^{aU} = [M_\mu]^{aL}$, $[M_\mu]^{bU} = [M_\mu]^{bL}$, $[M_\mu]^{cU} = [M_\mu]^{cL}$.
Now let us impose the following conditions:

- $F_{1U}^{'} = F_{1L}^{'}, F_{1U}^{''} = F_{1L}^{''}, F_{2U}^{'} = F_{2L}^{'}, F_{2U}^{''} = F_{2L}^{''}$, $F_{3U}^{'} = F_{3L}^{'}, F_{3U}^{''} = F_{3L}^{''}$ (continuity of the **H** tangential component)
- $\Phi_{1U}^{'} + \Phi_{1L}^{'} = \Phi_1^{'}$, $\Phi_{1U}^{''} + \Phi_{1L}^{''} = \Phi_1^{''}$, $\Phi_{2U}^{'} + \Phi_{2L}^{'} = \Phi_2^{'}$, $\Phi_{2U}^{''} + \Phi_{2L}^{''} = \Phi_2^{''}$,
  $\Phi_{3U}^{'} + \Phi_{3L}^{'} = \Phi_3^{'}$, $\Phi_{3U}^{''} + \Phi_{3L}^{''} = \Phi_3^{''}$ (additivity of the **B** flux)

Defining:
$[M_\mu]^a = 2\,[M_\mu]^{aU} = 2\,[M_\mu]^{aL}$, $[M_\mu]^b = 2\,[M_\mu]^{bU} = 2\,[M_\mu]^{aL}$, $[M_\mu]^c = 2\,[M_\mu]^{cU} = 2\,[M_\mu]^{aL}$ we can bring together each upper microcell with its respective lower microcell, achieving new bigger units. The new bigger unit constitutive equations are:

$$\begin{array}{l} \left\{ \begin{array}{c} \Phi_1^{''} \\ \Phi_2^{'} \end{array} \right\} = [M_\mu]^a \left\{ \begin{array}{c} F_1^{''} \\ F_2^{'} \end{array} \right\}, \\ \left\{ \begin{array}{c} \Phi_2^{''} \\ \Phi_3^{'} \end{array} \right\} = [M_\mu]^b \left\{ \begin{array}{c} F_2^{''} \\ F_3^{'} \end{array} \right\}, \\ \left\{ \begin{array}{c} \Phi_3^{''} \\ \Phi_1^{'} \end{array} \right\} = [M_\mu]^c \left\{ \begin{array}{c} F_3^{''} \\ F_1^{'} \end{array} \right\} \end{array} \quad (28)$$

This process of bringing together is possible only in particular cases as this one. In three-dimensional, more general cases, this is not possible. Let us assume that:

- $F_1^{'} = F_1^{''}, F_2^{'} = F_2^{''}, F_3^{'} = F_3^{''}$,
  (continuity of the **H** tangential component)
- $\Phi_1^{'} + \Phi_1^{''} = \Phi_1, \Phi_2^{'} + \Phi_2^{''} = \Phi_2, \Phi_3^{'} + \Phi_3^{''} = \Phi_3$,
  (additivity of the **B** flux)

Respecting the flux additivity condition, the continuity condition of the **B** normal component is automatically satisfied. With the continuity

condition and constitutive equations we can obtain the final magnetic constitutive equation on the primal cell:

$$\left\{ \begin{array}{c} \Phi_1 \\ \Phi_2 \\ \Phi_3 \end{array} \right\} = \left[\left[\begin{array}{ccc} M^a_{\mu 11} & M^a_{\mu 12} & 0 \\ M^a_{\mu 21} & M^a_{\mu 22} & 0 \\ 0 & 0 & 0 \end{array} \right] + \left[\begin{array}{ccc} 0 & 0 & 0 \\ 0 & M^b_{\mu 11} & M^b_{\mu 12} \\ 0 & M^b_{\mu 21} & M^b_{\mu 22} \end{array} \right] + \left[\begin{array}{ccc} M^c_{\mu 22} & 0 & M^c_{\mu 21} \\ 0 & 0 & 0 \\ M^c_{\mu 12} & 0 & M^c_{\mu 11} \end{array} \right] \right] \left\{ \begin{array}{c} F_1 \\ F_2 \\ F_3 \end{array} \right\} \tag{29}$$

that is:

$$\left\{ \begin{array}{c} \Phi_1 \\ \Phi_2 \\ \Phi_3 \end{array} \right\} = [M_\mu] \left\{ \begin{array}{c} F_1 \\ F_2 \\ F_3 \end{array} \right\} \tag{30}$$

In a synthetic notation we can rewrite the previous equation as:

$$\{\Phi\} = [M_\mu]\{F\} \tag{31}$$

Starting from (31), for a prismatic primal cell with triangular base, it is possible to demonstrate that the magnetic field must be uniform in each primal cell.

4.5.2. Electric Constitutive Equation

On the basis of the same considerations it is possible to obtain an analogous expression, on the dual cell, for the electric constitutive equation. Let us consider a three-dimensional primal cell as that in figure 12a, part of a two-dimensional extrude grid.

We assume that

- The field vectors **E** and **D** have only x and y-components and they are z-coordinate independent (two-dimensional fields).
- The dielectric constant ε is z-coordinate independent.

Thus, using the tensorial equation $\mathbf{D} = \varepsilon\mathbf{E}$, for the dual cell, we want to express the electric constitutive equation in the following form:

$$\left\{ \begin{array}{l} \Psi_1 = f_1(V_1, V_2, ..., V_6) \\ \Psi_2 = f_2(V_1, V_2, ..., V_6) \\ ... \\ \Psi_6 = f_6(V_1, V_2, ..., V_6) \end{array} \right. \tag{32}$$

where

- The variables Ψ are associated to the dual lateral surfaces $\tilde{S}$ (the Ψ associated to dual surfaces $\tilde{S}$ z-orthogonal are null).

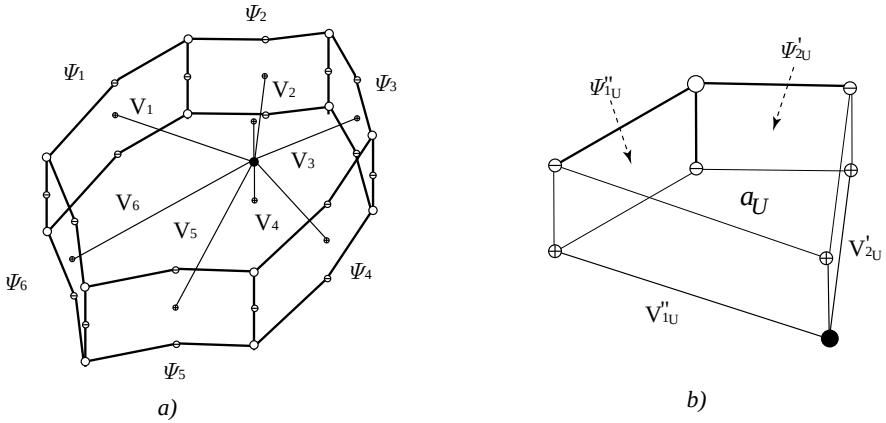

Figure 12. Dual two-dimensional extrude cell and one of its microcells.

- The variables V are associated to the parts of primal lines lying in the dual cell (the F associated to dual lines $\tilde{L}$ z-parallel are null).

Let us divide the dual cell in 12 microcells. For the microcell aU in figure (12b) we immediately obtain the constitutive equation for it:

$$\left\{ \begin{array}{c} \Psi''_{1U} \\ \Psi'_{2U} \end{array} \right\} = \left[\begin{array}{cc} \tilde{S}''_{1Ux} & \tilde{S}''_{1Uy} \\ \tilde{S}'_{2Ux} & \tilde{S}'_{2Uy} \end{array} \right] \varepsilon \left[\begin{array}{cc} L''_{1Ux} & L''_{1Uy} \\ L'_{2Ux} & L'_{2Uy} \end{array} \right]^{-1} \left\{ \begin{array}{c} V''_{1U} \\ V'_{2U} \end{array} \right\} \quad (33)$$

or

$$\left\{ \begin{array}{c} \Psi''_{1U} \\ \Psi'_{2U} \end{array} \right\} = [M_\varepsilon]^{aU} \left\{ \begin{array}{c} V''_{1U} \\ V'_{2U} \end{array} \right\} \quad (34)$$

In this way, with the same assumptions, we can express the constitutive equations of all the microcells in the dual cell. Since each upper microcell (U) is equal to its respective lower microcell (L) we can bring together each upper microcell with its respective lower microcell, achieving new bigger units. The new bigger unit constitutive equations are:

$$
\begin{aligned}
\left\{ \begin{array}{c} \Psi_1^{''} \\ \Psi_2^{'} \end{array} \right\} &= [M_\varepsilon]^a \left\{ \begin{array}{c} V_1^{''} \\ V_2^{'} \end{array} \right\}, \\
\left\{ \begin{array}{c} \Psi_2^{''} \\ \Psi_3^{'} \end{array} \right\} &= [M_\varepsilon]^b \left\{ \begin{array}{c} V_2^{''} \\ V_3^{'} \end{array} \right\}, \\
\left\{ \begin{array}{c} \Psi_3^{''} \\ \Psi_4^{'} \end{array} \right\} &= [M_\varepsilon]^c \left\{ \begin{array}{c} V_3^{''} \\ V_4^{'} \end{array} \right\}, \\
\left\{ \begin{array}{c} \Psi_4^{''} \\ \Psi_5^{'} \end{array} \right\} &= [M_\varepsilon]^d \left\{ \begin{array}{c} V_4^{''} \\ V_5^{'} \end{array} \right\}, \\
\left\{ \begin{array}{c} \Psi_5^{''} \\ \Psi_6^{'} \end{array} \right\} &= [M_\varepsilon]^e \left\{ \begin{array}{c} V_5^{''} \\ V_6^{'} \end{array} \right\}, \\
\left\{ \begin{array}{c} \Psi_6^{''} \\ \Psi_1^{'} \end{array} \right\} &= [M_\varepsilon]^f \left\{ \begin{array}{c} V_6^{''} \\ V_1^{'} \end{array} \right\}
\end{aligned}
\tag{35}
$$

Let us assume that:

- $V_1^{'} = V_1^{''}, V_2^{'} = V_2^{''}, ..., V_6^{'} = V_6^{''}$,
  (continuity of the tangential component of $\mathbf{E}$)
- $\Psi_1^{'} + \Psi_1^{''} = \Psi_1, \Psi_2^{'} + \Psi_2^{''} = \Psi_2, \Psi_3^{'} + \Psi_3^{''} = \Psi_3$,
  (additivity of the $\mathbf{D}$ flux)

Respecting the flux additivity condition, the continuity condition of the $\mathbf{D}$ normal component is automatically satisfied . With the continuity condition and constitutive equations we can obtain the final electric constitutive equation on the dual cell:

$$
\begin{aligned}
\left\{ \begin{array}{c} \Psi_1 \\ \Psi_2 \\ \Psi_3 \\ \Psi_4 \\ \Psi_5 \\ \Psi_6 \end{array} \right\} = \Bigg[\Bigg[\begin{bmatrix} M^a_{\varepsilon\,11} & M^a_{\varepsilon\,12} & 0 & 0 & 0 & 0 \\ M^a_{\varepsilon\,21} & M^a_{\varepsilon\,22} & 0 & 0 & 0 & 0 \\ 0 & 0 & 0 & 0 & 0 & 0 \\ 0 & 0 & 0 & 0 & 0 & 0 \\ 0 & 0 & 0 & 0 & 0 & 0 \\ 0 & 0 & 0 & 0 & 0 & 0 \end{bmatrix} + \begin{bmatrix} 0 & 0 & 0 & 0 & 0 & 0 \\ 0 & M^b_{\varepsilon\,11} & M^b_{\varepsilon\,12} & 0 & 0 & 0 \\ 0 & M^b_{\varepsilon\,21} & M^b_{\varepsilon\,22} & 0 & 0 & 0 \\ 0 & 0 & 0 & 0 & 0 & 0 \\ 0 & 0 & 0 & 0 & 0 & 0 \\ 0 & 0 & 0 & 0 & 0 & 0 \end{bmatrix} \\
+ ... + \begin{bmatrix} M^f_{\varepsilon\,22} & 0 & 0 & 0 & 0 & M^f_{\varepsilon\,21} \\ 0 & 0 & 0 & 0 & 0 & 0 \\ 0 & 0 & 0 & 0 & 0 & 0 \\ 0 & 0 & 0 & 0 & 0 & 0 \\ 0 & 0 & 0 & 0 & 0 & 0 \\ M^f_{\varepsilon\,12} & 0 & 0 & 0 & 0 & M^f_{\varepsilon\,11} \end{bmatrix} \Bigg] \Bigg] \left\{ \begin{array}{c} V_1 \\ V_2 \\ V_3 \\ V_4 \\ V_5 \\ V_6 \end{array} \right\}
\end{aligned}
\tag{36}
$$

that is

$$\begin{Bmatrix} \Psi_1 \\ \Psi_2 \\ \Psi_3 \\ \Psi_4 \\ \Psi_5 \\ \Psi_6 \end{Bmatrix} = [M_\varepsilon] \begin{Bmatrix} V_1 \\ V_2 \\ V_3 \\ V_4 \\ V_5 \\ V_6 \end{Bmatrix} \tag{37}$$

In a synthetic notation we can rewrite the previous equation as:

$$\{\Psi\} = [M_\varepsilon]\{V\} \tag{38}$$

In this case the dimension of matrix M_ε, that is the number of microcell pair in the dual cell, is not 3 but it depends from the number of primal points that lie on the border of the dual cell. This number, in this case, goes generally from 4 to 8.

4.5.3. Ohm's Law

For a generic dual cell we can obtain the electric constitutive equation:

$$\{\Psi\}^{n+1/2} = [M_\varepsilon]\{V\}^{n+1/2} \tag{39}$$

Ohm's law is obtainable in the same way as (39) substituting:

- The variable $\{I_\mathrm{c}\}^n$ with $\{\Psi\}^{n+1/2}$,
- The tensor σ with the tensor ε e
- The variable $\frac{\{V\}^{n+1/2}+\{V\}^{n-1/2}}{2}$ with $\{V\}^{n+1/2}$.

Accordingly Ohm's law is:

$$\{I_\mathrm{c}\}^n = [M_\sigma]\frac{\{V\}^{n+1/2} + \{V\}^{n-1/2}}{2} \tag{40}$$

4.6. Considerations on Maxwell-Ampère's Law

Using the electric constitutive equation (39) and the Ohm's law (40) it is possible to obtain an explicit expression for Maxwell-Ampère's law. Given a dual cell, for each dual surface $\tilde{\mathbf{s}}_\alpha$ the law is

$$\Psi_\alpha^{n+1/2} = \Psi_\alpha^{n-1/2} + \tilde{\tau}_n \sum_\beta \tilde{c}_{\alpha\beta} F_\beta^n - \tilde{\tau}_n (I_{\mathrm{c}\alpha}^n + I_{\mathrm{i}\alpha}^n) \tag{41}$$

Defining an auxiliary variable as follows:

$$\overline{\Psi}_\alpha^{n+1/2} = \overline{\Psi}_\alpha^{n-1/2} + \tilde{\tau}_n \sum_\beta \tilde{c}_{\alpha\beta} F_\beta^n \tag{42}$$

for every dual surface $\tilde{\mathbf{s}}_\alpha$, the Maxwell-Ampère's law becomes:

$$\Psi_\alpha^{n+1/2} = \Psi_\alpha^{n-1/2} + (\overline{\Psi}_\alpha^{n+1/2} - \overline{\Psi}_\alpha^{n-1/2}) - \tilde{\tau}_n(I_{\mathrm{c}\alpha}^{\,n} + I_{\mathrm{i}\alpha}^{n}) \tag{43}$$

or, on the dual cell:

$$\{\Psi\}^{n+1/2} = \{\Psi\}^{n-1/2} + (\{\overline{\Psi}\}^{n+1/2} - \{\overline{\Psi}\}^{n-1/2}) - \tilde{\tau}_n(\{I_{\mathrm{c}}\}^n + \{I_{\mathrm{i}}\}^n) \tag{44}$$

Since, for Ohm's law (40) and for electric constitutive equation (39), it is:

$$\{I_{\mathrm{c}}\}^n = \frac{1}{2}[M_\sigma][M_\varepsilon]^{-1}(\{\Psi\}^{n+1/2} + \{\Psi\}^{n-1/2}) \tag{45}$$

using (45) into (44) we can achieve an explicit expression for Ψ:

$$\begin{aligned} &\{\Psi\}^{n+1/2} = \\ &\left[[I] + \frac{\tilde{\tau}_n}{2}[M_\sigma][M_\varepsilon]^{-1}\right]^{-1}\left[[I] - \frac{\tilde{\tau}_n}{2}[M_\sigma][M_\varepsilon]^{-1}\right]\{\Psi\}^{n-1/2} + \\ &\left[[I] + \frac{\tilde{\tau}_n}{2}[M_\sigma][M_\varepsilon]^{-1}\right]^{-1}(\{\overline{\Psi}\}^{n+1/2} - \{\overline{\Psi}\}^{n-1/2} - \tilde{\tau}_n\{I_{\mathrm{i}}\}^n) \end{aligned} \tag{46}$$

or, if we are interested in knowing the voltages V on the parts of primal lines inside the primal cell, we use the following:

$$\begin{aligned} \{V\}^{n+1/2} = &\left[\frac{[M_\varepsilon]}{\tilde{\tau}_n} + \frac{[M_\sigma]}{2}\right]^{-1}\left[\frac{[M_\varepsilon]}{\tilde{\tau}_n} - \frac{[M_\sigma]}{2}\right]\{V\}^{n-1/2} + \\ &\left[\frac{[M_\varepsilon]}{\tilde{\tau}_n} + \frac{[M_\sigma]}{2}\right]^{-1}\frac{1}{\tilde{\tau}_n}(\{\overline{\Psi}\}^{n+1/2} - \{\overline{\Psi}\}^{n-1/2} - \tilde{\tau}_n\{I_{\mathrm{i}}\}^n) \end{aligned} \tag{47}$$

In order to obtain the voltages on primal lines it is necessary to perform a sum of the voltages of their two parts belonging to two distinct dual cells. Now let us observe that:

- Maxwell-Ampère's law (46) is similar to the analogous equation for the Delaunay-Voronoi method (18) and to the FDTD method [11].
- If the medium is isotropic and homogeneous in ε e σ inside a dual cell, then the material matrices for the dual cell are $[M_\varepsilon] = [M]\varepsilon$ and $[M_\sigma] = [M]\sigma$ with $[M]$ square invertible matrix. Using (39) with (40), we obtain:

$$\{I_{\mathrm{c}}\}^n = \frac{\sigma}{\varepsilon}\frac{\{\Psi\}^{n+1/2} + \{\Psi\}^{n-1/2}}{2} \tag{48}$$

which is the simple relation

$$I_\alpha^n = \frac{\sigma}{2\varepsilon}(\Psi_\alpha^{n+1/2} + \Psi_\alpha^{n+1/2}) \tag{49}$$

on the dual surfaces $\tilde{\mathbf{s}}_\alpha$. In this case the vectorial Maxwell-Ampère's law (46) can be broken down into a set of equations as (18).

4.7. Computational Algorithm

Starting from initial conditions as:
$I_\alpha^{-1} = 0$, $V_\alpha^{-1/2} = 0 \Rightarrow \Psi_\alpha^{-1/2} = 0$, $F_\beta^0 = 0 \Rightarrow \Phi_\beta^0 = 0$
the variables of the electrodynamic field, generated by an impressed current starting from the initial time instant $n = 0$, can be computed through the following steps:

- Computation of $\{\Psi\}^{1/2}$, for every dual cell, by the Maxwell-Ampère's law (46).
- Computation of $\{V\}^{1/2}$, for every dual cell, by the electric constitutive equation (38) and any given boundary conditions. Then it is necessary to reassemble all $\{V\}^{1/2}$ on primal lines by summing the voltages on their parts.
- Computation of $\{\Phi\}^1$, for every primal cell, by the Faraday's law (6).
- Computation of $\{F\}^1$ by the magnetic constitutive equation (31) and by any given boundary conditions. Then it is necessary to reassemble all $\{F\}^1$ on dual lines by summing the voltages on their parts.
- Iterate

4.8. Considerations on Microcell Method

Referring to the introductory demands, we can illustrate some general results that we do not demonstrate here:

(i) Microcell method is applicable to many kind of grids, structured or not, having cells with various shapes. This satisfies items (i) and (ii).
(ii) On Cartesian orthogonal grids, with primal cells ε and σ homogeneous and dual cells μ homogeneous, the microcell method leads to the same equations as FDTD method. This satisfies item (iii).
(iii) Using the Microcell Method on the Delaunay-Voronoi grids, in all two-dimensional non degenerate cases, we can obtain the same equations as Delaunay-Voronoi Method.
(iv) Using barycentric grids we have eliminated all the problems of Delaunay-Voronoi Method related to the primal cell shapes.

(v) Item (iv) is satisfied by the particular form of electrodynamic equations.
(vi) The theoretical and experimental validity of equation (9), at least in its simplest forms, satisfies item (v).
(vii) The constitutive equations defined in the cells are a global version of the tensorial relations between the field variables.
(viii) Using the Microcell Method we can study isotropic and non-isotropic cases in the same way.

5. COMPUTATIONAL ASPECTS OF THE CELL METHOD

In order to value some computational aspects of the Cell Method, we propose to solve two simple two-dimensional problems, the former the dual of the latter, with both the FDTD and microcell time-domain (MCTD) methods.

5.1. Problem 1

Let us consider a closed, three-dimensional rectangular resonant cavity, made by a perfect electric conductor, with sizes a=0.1 m, b=0.1 m, h=0.001 m. It is supplied by a coaxial cable, with a small thickness, lying long the axes z in x_0=0.02 m, y_0=0.02 m.

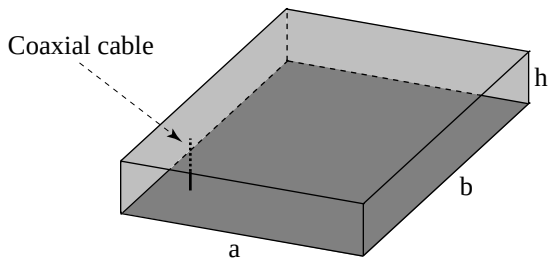

Figure 13. Resonant cavity.

Moreover we suppose that the feed signal is an electric current impulse as:

$$I = I_0 \exp\left\{-\frac{(t-t_0)^2}{2T^2}\right\} \tag{50}$$

where I_0=1 A, T=32 ps and t_0=3T. Let us compute:

(i) Input voltage, in the feed point, in the periods 1–200 ps, 1–4000 ps, 4001–8000 ps assuming that the resonant cavity is homogeneous and lossless (free-space).
(ii) Input voltage, in the feed point, in the periods 1–4000 ps, 4001–8000 ps, 1–16384 ps assuming that the resonant cavity is homogeneous with a medium of conductivity σ=5e-3 S .
(iii) Input impedance of the cavity in the case of item 2, in magnitude and phase, in the range 0–6 GHz.

Since the height of the cavity is low compared to the wavelength, we can assume only the presence of TM modes in the cavity.

5.1.1. Numerical Modeling of Problem 1

We will use the FDTD and MCTD methods to find the solutions to items (i), (ii), (iii). Moreover, for item (iii), we will also use the resonant cavity method [3].

FDTD Method

The main features are:

(i) Number of Yee's cells: $N = Nx = Ny = 50,\ Nz = 1$ (Total number of cells $(N+1)^2 = 2601$).
(ii) Sizes of Yee's cells: $\Delta x = \Delta y = 0.002$ m, $\Delta z = 0.001$ m.
(iii) Time step $\tau = 1$ ps.
(iv) Number of time steps $Nc = 16384$.

Assuming only the presence of TM modes in the cavity, at each computational step we must compute 2500 values of E_z, and 5100 values of H_x and H_y together.

MCTD Method

We can solve the problem using a triangular primal grid and a barycentric dual grid, both of them two-dimensional, as those in figure 14:
The grid contains:

(i) Number of primal cells = Number of surfaces $S = N_S$=1219.
(ii) Number of dual cells = Number of surfaces $\tilde{S} = N_{\tilde{S}}$= 648.

The resulting primal and dual two-dimensional extrude grids are shown in figure 15.

(a) Magnetic constitutive equation.
Since the magnetic field has only x and y components, the constitutive magnetic equation we use is (31).

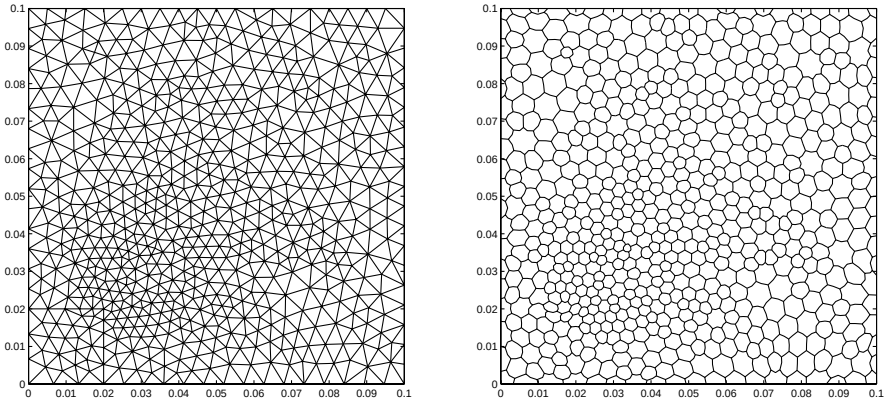

Figure 14. Delaunay-barycentric grids

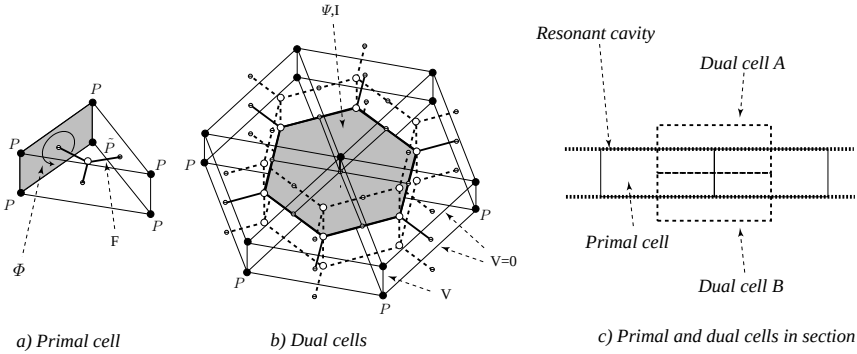

Figure 15. TM case.

(b) Electric constitutive equation.
In order to obtain the constitutive electric equation, we must observe that in this case, for the lower microcell (L) of the dual cell A in figure (16), is:

$$\Psi_{1Aa} = \varepsilon \frac{V_{AL}}{l_{AL}} \tilde{s}_{1a} \tag{51}$$

Since the electric field has only z-components and since all the lower microcells of A have the same voltage V_{AL}, inside them there is the

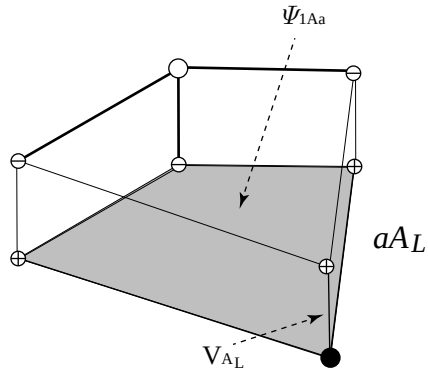

Figure 16. Microcell Aa_L.

same uniform electric field. Thus, for the lower half of A we can write:

$$\Psi_{1A} = \sum_a \Psi_{1Aa} = \varepsilon \frac{V_{AL}}{l_{AL}} \sum_a \tilde{s}_{1a} = \varepsilon \frac{V_{AL}}{l_{AL}} \tilde{s}_1 \tag{52}$$

With analogous considerations, for the upper half of the dual cell B the electric constitutive equation is:

$$\Psi_{1B} = \sum_a \Psi_{1Ba} = \varepsilon \frac{V_{BU}}{l_{BU}} \sum_a \tilde{s}_{1a} = \varepsilon \frac{V_{BU}}{l_{BU}} \tilde{s}_1 \tag{53}$$

In order to satisfy the continuity we must impose that: $\Psi_{1A} = \Psi_{1B}$ Defining $V_1 = V_{AL} + V_{BU}$,$L_1 = L_{AL} + L_{BU}$ and putting together the lower microcells of A with the upper microcells of B, we obtain a new unit in which the electric field is uniform; its electric constitutive equation is:

$$\Psi_1 = \varepsilon \frac{V_1}{l_1} \tilde{s}_1 \tag{54}$$

that is the same of the Delaunay-Voronoi method since the same assumptions are verified.

(c) Ohm's law.
In the same way, we can express Ohm's law by means of (12) or, in a more direct manner, by (16).

Other observations are:

(i) In the resonant cavity, **H** field is approximated by 1219 (=number of primal cells) uniform fields, while **E** field is approximated by 648 (=number of dual cells) uniform fields.

(ii) At each time step we should compute 1866 Φ values by (6), 3*1219=3657 F values by (31) and 648 V values using a simple form of (47). In practice, it is not necessary to compute Ψ and I_c because they are not used in the update.
(iii) In order to satisfy the boundary conditions, we may impose that V is zero on all the transverse primal lines L and on all the vertical ones lying on the border of cavity.
(iv) The primal feed point (where we calculate the output voltage signal) is (0.02,0.02).

In order to ensure the numerical stability of the leap-frog algorithm, τ must be upper limited by:

$$\tau \leq min_\beta \left(\frac{1}{c_\beta} \sqrt{\frac{2s_\beta}{\sum_\beta |c_{\alpha\beta}| \frac{l_\alpha}{\tilde{l}_\alpha}}} \right) \tag{55}$$

where c_β is the maximum speed of waves in the primal cells s_β. This case (55) imposes $\tau \leq 4.89$ ps while, in some computations, we have found that instability arises by $\tau \geq 5.64$ ps. So we assume:

(i) Time step τ=1ps.
(ii) Number of steps Nc=16384.

Resonant cavity method

The impedance in the feed point is computable by the theoretical formula:

$$Z = j\omega\mu\Delta z \frac{4}{ab} \sum_{m=1}^{\infty} \sum_{n=1}^{\infty} \frac{\sin(k_m x_0)^2 \sin(k_n y_0)^2}{{k_{mn}}^2 - {k_c}^2} \left(\frac{\sin\left(\frac{k_m dx}{2}\right)}{\frac{k_m dx}{2}} \right)^2 \tag{56}$$

where: $k_m = \frac{m\pi}{a}$, $k_n = \frac{n\pi}{b}$, ${k_{mn}}^2 = {k_m}^2 + {k_n}^2$, ${k_c}^2 = k^2 \left(1 - j\frac{\sigma}{\omega\varepsilon}\right)$. In practice the sum is extended till $m = n = 100$. Moreover the quantity dx is the thickness of the coaxial cable. We assume dx=0.002 m.

5.2. Problem 2

Let us consider a closed, three-dimensional rectangular resonant cavity, made by a perfect magnetic conductor, with dimensions $a = 0.1$ m,

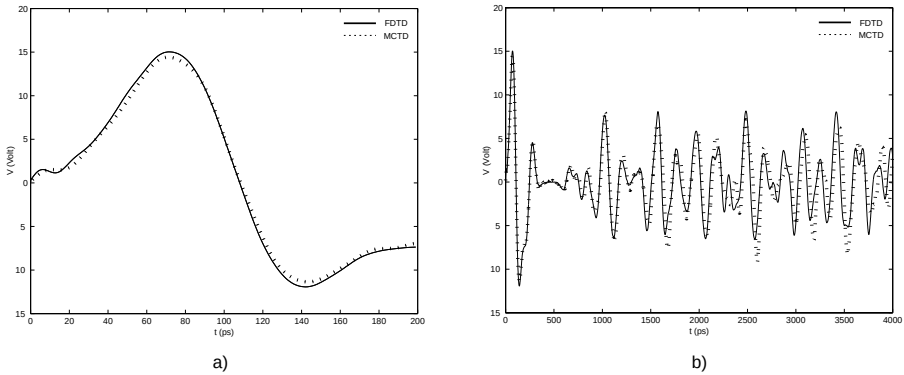

Figure 17. a) Item (i): Electric input voltage in the period 1-200 ps, b) Item (i): Electric input voltage in the period 1–4000 ps.

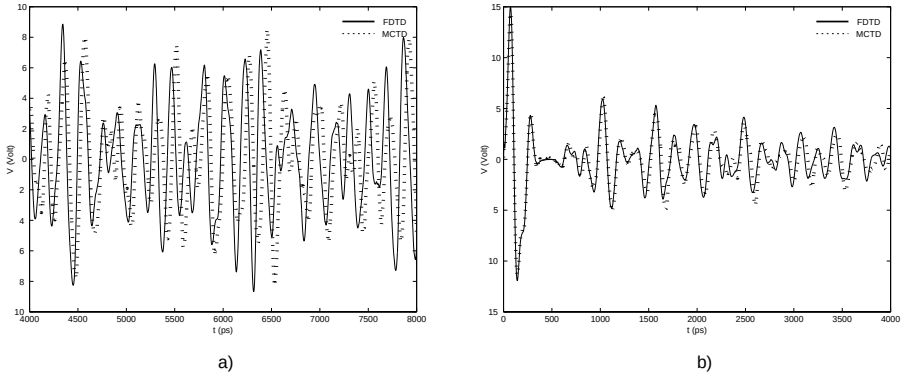

Figure 18. a) Item (i): Electric input voltage in the period 4001–8000 ps, b) Item (ii): Electric input voltage in the period 1–4000 ps.

$b = 0.1$ m, $h = 0.001$ m. We assume that a magnetic current impulse is supplied [11] as:

$$M = M_0 \exp\left(-\frac{(t-t_0)^2}{2T^2}\right) \tag{57}$$

where M_0= 1 V, T=32 ps and t_0=3T. The term $M_{i\beta}^{n+1/2}$, multiplied for τ_n must be subtracted from the second part of Faraday's law (6). Let us compute:

(i) Input magnetic voltage, in the feed point, in the periods 1–200

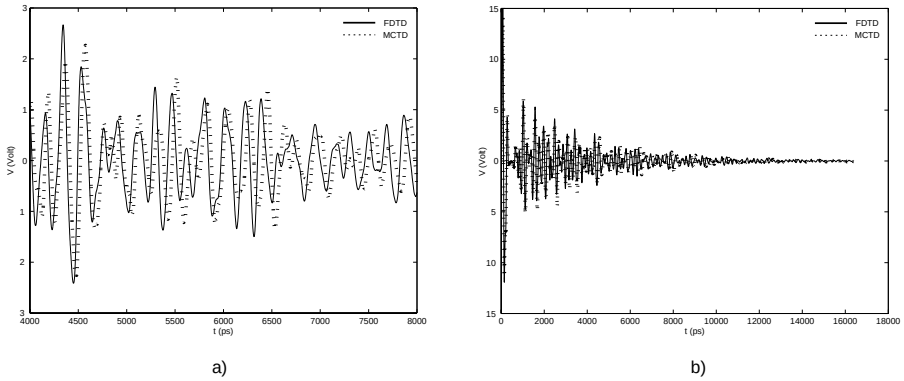

Figure 19. a) Item (ii): Electric input voltage in the period 4001–8000 ps, b) Item (ii): Electric input voltage in the period 1–16384 ps.

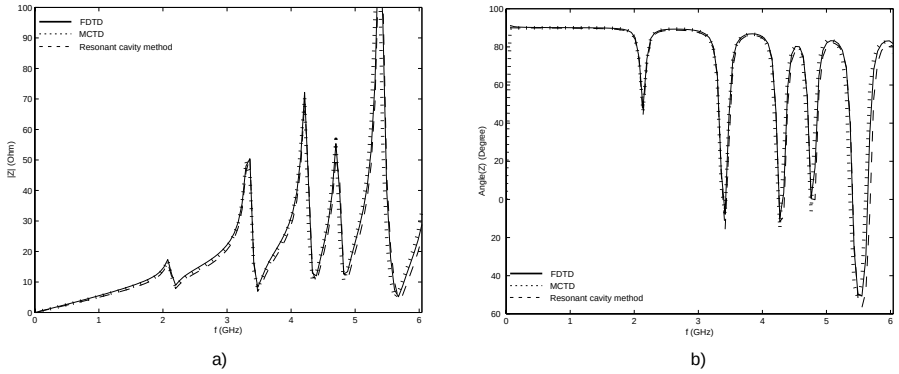

Figure 20. a) Item (iii): Module of the input impedance in the range 0–6 GHz, b) Item (iii): Phase of the input impedance in the range 0–6 GHz.

ps, 1–4000 ps, 4001–8000 ps assuming that the resonant cavity is homogeneous and lossless (free-space).

(ii) Input magnetic voltage, in the feed point, in the periods 1–4000 ps, 4001–8000 ps, 1–16384 ps assuming that the resonant cavity is homogeneous with a medium of conductivity σ=5e-3 s.

Since the height of the cavity is small in comparison to the wavelength, we may assume the presence of only TE modes in the cavity.

5.2.1. Numerical Modeling of Problem 2

We will use only the FDTD and MCTD methods to find the solutions to items (i) and (ii).

FDTD Method

The main features are the same as in problem 1. The only differences are that, assuming the presence of only TE modes in the cavity, at each computational step we must compute 2500 values of H_z, and 5100 values of E_x and E_y together.

MCTD Method

Primal and dual grids are the same as problem 1 and the resulting two-dimensional extrude cells are shown in figure 21.

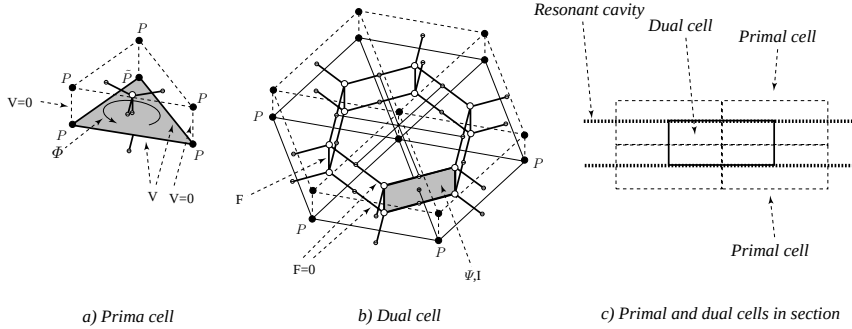

Figure 21. TE case

(a) Magnetic constitutive equation.
The magnetic constitutive equation is (10), obtainable in the same way as we obtained the electric constitutive equation in the previous paragraph.

(b) Electric constitutive equation.
Since the electric field has only x and y components, the electric constitutive equation is (38).

(c) Ohm's law.
As for electric constitutive equations, Ohm's law is obtained, on dual cells, by using equation (40).

Other observations are:

(i) In the cavity, the **H** field is approximated by 1219 (= primal cells number) uniform fields, while the **E** field is approximated by 3657 (= pair of microcells number) uniform fields.

(ii) At each computational step we should compute 1219 F values by (6), (10), 3732 V values using (47). In practice it is not necessary to compute the Φ values because the equation (6) can be resolved directly in function of F and M impressed. Everything is analogous for the Ψ values.

(iii) To satisfy the boundary conditions we must impose F=0 on all the primal transverse dual lines L and on all the vertical ones lying on the border of cavity. Yet there are no vertical dual lines on the border: where do we have to impose F=0 ? Let us take a dual cell at the border, as that in figure 22. This cell is not equal to

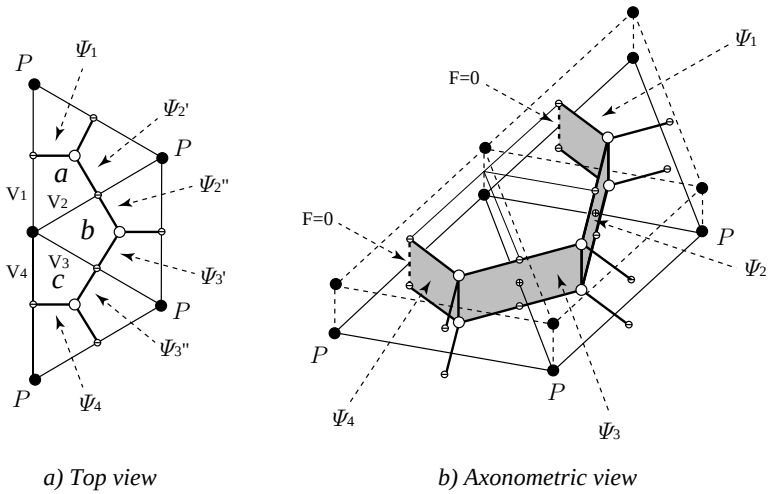

Figure 22. Boundary conditions.

the other dual cells inside the domain. Nevertheless, we can apply the Microcell method to obtain the electric constitutive equation:

$$\left\{\begin{array}{c}\Psi_1\\ \Psi_2\\ \Psi_3\\ \Psi_4\end{array}\right\} = \left[\left[\begin{array}{cccc} {M_{\varepsilon 11}}^a & {M_{\varepsilon 12}}^a & 0 & 0\\ {M_{\varepsilon 21}}^a & {M_{\varepsilon 22}}^a & 0 & 0\\ 0 & 0 & 0 & 0\\ 0 & 0 & 0 & 0\end{array}\right] + \left[\begin{array}{cccc} 0 & 0 & 0 & 0\\ 0 & {M_{\varepsilon 11}}^b & {M_{\varepsilon 12}}^b & 0\\ 0 & {M_{\varepsilon 21}}^b & {M_{\varepsilon 22}}^b & 0\\ 0 & 0 & 0 & 0\end{array}\right] + \left[\begin{array}{cccc} 0 & 0 & 0 & 0\\ 0 & 0 & 0 & 0\\ 0 & 0 & {M_{\varepsilon 11}}^c & {M_{\varepsilon 12}}^c\\ 0 & 0 & {M_{\varepsilon 21}}^c & {M_{\varepsilon 22}}^c\end{array}\right]\right] \left\{\begin{array}{c}V_1\\ V_2\\ V_3\\ V_4\end{array}\right\} \tag{58}$$

where Ψ_1 and Ψ_4 are computed by means of a F circulation between the inside part and the outside part of the border. In this case, we impose that $F = 0$ outside the border to satisfy our boundary condition.

(iv) The dual feed point (and where we take the out signal) is the nearest dual point to (0.02,0.02). The point we choose is (0.0206,0.0215).

In order to assure the numerical stability of leap-frog algorithm, τ must be upper limited by:

$$\tau \leq min_\alpha \left(\frac{1}{c_\alpha} \sqrt{\frac{2\tilde{s}_\alpha}{\sum_\beta |\tilde{c}_{\beta\alpha}| \frac{\tilde{l}_\beta}{l_\beta}}} \right) \tag{59}$$

where c_α is the maximum speed of waves in the dual cells $\tilde{s}_\alpha$. In this case, this formula imposes $\tau \leq 3.25$ ps while, in some computations, we have found instability for $\tau \geq 3.33$ ps.

5.3. Summary of Numerical Results

Problem 1

The input voltage curves, obtained by FDTD and MCTD methods, are quite similar during a period of about 1000 ps. Beyond this period it is possible to note a small dispersion. The reason for this is that the discretization of the FDTD method in these examples is actually much finer than that of MCTD method. In fact, the FDTD method approximates the **E** and **H** fields in the cavity with 2500 and 10000 uniform fields, while the MCTD method uses 648 and 1219 uniform fields. We obtain a good approximation between the impedance values too, so we can see that with the MCTD method we have obtained good

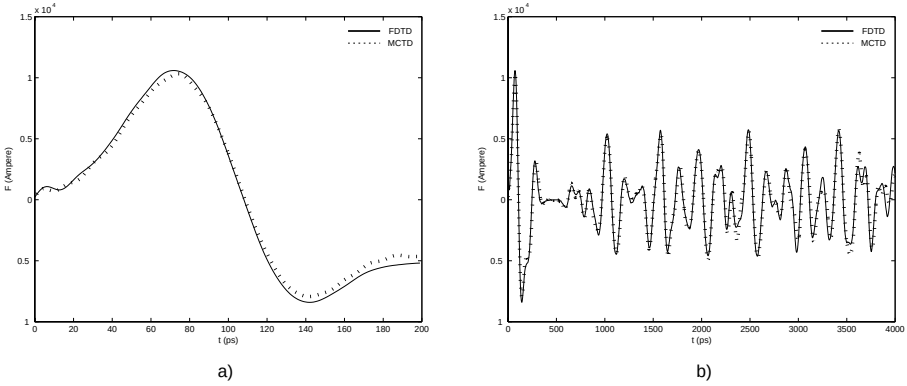

Figure 23. a) Item (i): Magnetic input voltage in the period 1–200 ps, b) Item (i): Magnetic input voltage in the period 1–4000 ps.

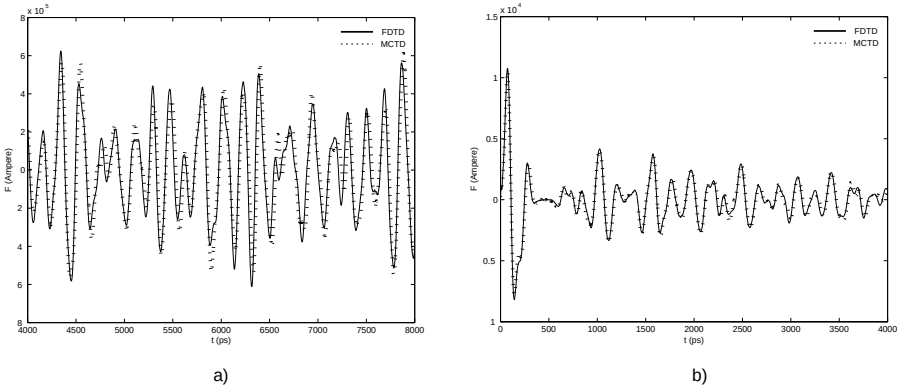

Figure 24. a) Item (i): Magnetic input voltage in the period 4001–8000 ps, b) Item (ii): Magnetic input voltage in the period 1–4000 ps.

results.
For our computations we have used a program written in C, running on a PENTIUM2-400 MHz. The computational time for the FDTD method was about 1 minute (for 7600 unknowns), while for the MCTD method it was about 4 minutes (for 6171 unknowns among V, F and Φ). Hence the FDTD method is about 5 times faster than the MCTD method for the computation of the same number of unknowns. However, this factor can be reduced by using some strategies to avoid recalculating many values at every step on the MCTD.

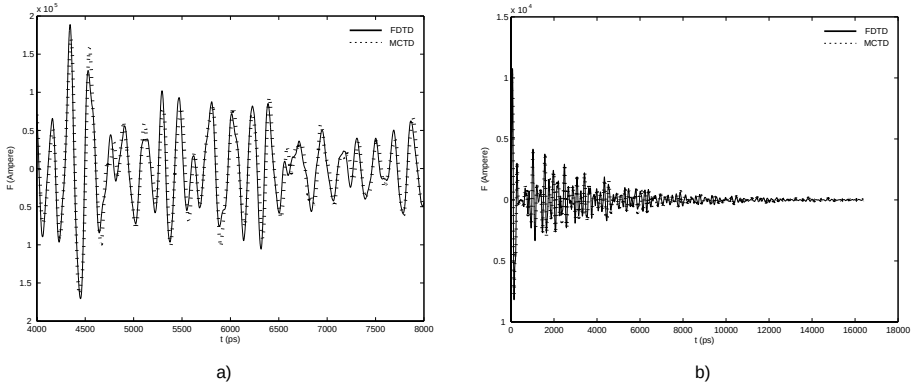

Figure 25. a) Item (ii): Magnetic input voltage in the period 4001–8000 ps, b) Item (ii): Magnetic input voltage in the period 1–16384 ps.

Problem 2
In the problem 2 the FDTD method approximates the **E** and **H** fields in the cavity with 10000 e 2500 uniform fields, while the MCTD method with 3657 and 1219 uniform fields . From the results achieved we can see that with an increase in the number of approximating fields (cells) in the MCTD method it is possible to have a better concordance with the the FDTD method results and less dispersion.

6. CONCLUSIONS

In this paper, we have analyzed some computational aspects of the Cell Method, in the version called *Microcell Method*. While in the paper [12] the finite formulation of electrodynamics was restricted to Delaunay-Voronoi grids, that restriction has been removed here so that we may employ more general grids. From the theory and from the results obtained it is possible to observe some significant aspects of the Cell Method. It is founded on a solid theoretical basis, and allows accurate results and the study of general structures. However, further theoretical studies and practical simulations are necessary to fully verify its applicability and to understand the real potential of this methodology.

REFERENCES

1. Pauli, W., *Elettrodinamica,* (translation of *Vorlesung Elektrodynamik*), Boringhieri (ed.), 1964.
2. Yee, K. S., "Numerical solution of initial boundary value problems involving Maxwell's equations in isotropic media," *IEEE Transactions on Antennas and Propagation,* Vol. 14, 302–307, 1966.
3. Carver, K. R. and J. W. Mink, "Microstrip antenna technology," *IEEE Transactions on Antennas and Propagation,* Vol. 29, 2–24, 1981.
4. Holland, R., "Finite difference solutions of Maxwell's equations in generalized nonorthogonal coordinates," *IEEE Transactions on Nuclear Science,* Vol. 30, No. 6, 4689–4591, 1983.
5. Fusco, M., "FDTD algorithm in curvilinear coordinates," *IEEE Transactions on Antennas and Propagation,* Vol. 38, No. 1, 76–89, 1990.
6. Lee, J. F., R. Palandech, and R. Mittra, "Modeling three-dimensional discontinuites in waveguides using nonorthogonal FDTD algorithm," *IEEE Transactions on Microwave and Techniques,* Vol. 40, No. 2, 346–352, 1992.
7. Lee, C. F., B. J. McCartin, R. T. Shin, and J. A. Kong, "A triangular-grid finite-difference time-domain method for electromagnetic scattering problems," *Journal of Electromagnetics Waves and Applications,* Vol. 8, No. 4, 449–470, 1994.
8. Madsen, N. K., "Divergence preserving discrete surface integral methods for Maxwell's curl equations using non-orthogonal unstructured grids," *Journal of Computational Physics,* Vol. 119, 34–45, 1995.
9. Hano, M. and T. Itoh, "Three-dimensional time-domain method for solving Maxwell's equations based on circumcenters of elements," *IEEE Transactions on Magnetics,* Vol. 32, No. 3, 946–949, 1996.
10. Schuhmann, R. and T. Weiland, "FDTD on nonorthogonal grids with triangular fillings," *IEEE Transactions on Magnetics,* Vol. 35, No. 3, 1470–1473, 1999.
11. Taflove, A., *Computational Electrodynamics: The Finite-Difference Time-Domain Method,* Artech House, 1995.
12. Tonti, E., "Finite formulation of the electromagnetic field," this volume.